Brain-Derived Neurotrophic Factor-Loaded Low-Temperature-Sensitive liposomes as a drug delivery system for repairing podocyte damage

Xiaoyi Huang [a,1,2], Min Li [b,2], Maria Isabel Martinez Espinoza [a], Cristina Zennaro [c], Fleur Bossi [c], Caterina Lonati [d], Samanta Oldoni [d], Giuseppe Castellano [e,f], Carlo Alfieri [e,f], Piergiorgio Messa [e,f], Francesco Cellesi [a,*]

[a] Dipartimento di Chimica, Materiali ed Ingegneria Chimica "G. Natta". Politecnico di Milano, Via Mancinelli 7, 20131 Milan, Italy
[b] Renal Research Laboratory, Fondazione IRCCS Ca' Granda Ospedale Maggiore Policlinico, Via Pace 9, 20122 Milan, Italy
[c] Department of Medical, Surgical and Health Sciences, University of Trieste, Cattinara Hospital, Strada di Fiume, 447, I 34149 Trieste, Italy
[d] Center for Preclinical Research, Fondazione IRCCS Ca' Granda - Ospedale Maggiore Policlinico, Milan, Italy
[e] Unit of Nephrology, Dialysis and Renal Transplant, Fondazione IRCCS Ca' Granda Ospedale Maggiore Policlinico Milan, Italy
[f] Department of Clinical Sciences and Community Health, University of Milan, Milan, Italy

A R T I C L E   I N F O

A B S T R A C T

Podocytes, cells of the glomerular filtration barrier, play a crucial role in kidney diseases and are gaining attention as potential targets for new therapies. Brain-Derived Neurotrophic Factor (BDNF) has shown promising results in repairing podocyte damage, but its efficacy via parenteral administration is limited by a short half-life. Low temperature sensitive liposomes (LTSL) are a promising tool for targeted BDNF delivery, preserving its activity after encapsulation. This study aimed to improve LTSL design for efficient BDNF encapsulation and targeted release to podocytes, while maintaining stability and biological activity, and exploiting the conjugation of targeting peptides. While cyclic RGD (cRGD) was used for targeting endothelial cells in vitro, a homing peptide (HITSLLS) was conjugated for more specific uptake by glomerular endothelial cells in vivo. BDNF-loaded LTSL successfully repaired cytoskeleton damage in podocytes and reduced albumin permeability in a glomerular co-culture model. cRGD conjugation enhanced endothelial cell targeting and uptake, highlighting an improved therapeutic effect when BDNF release was induced by thermoresponsive liposomal degradation. In vivo, targeted LTSL showed evidence of accumulation in the kidneys, and their BDNF delivery decreased proteinuria and ameliorated kidney histology. These findings highlight the potential of BDNF-LTSL formulations in restoring podocyte function and treating glomerular diseases.

1. Introduction

Current treatments for managing or mitigating kidney damage often suffer from adverse side effects and limited efficacy(Whittaker et al., 2018). To tackle this problem, it is crucial to develop targeted therapies that deliver drugs in a selective manner to increase efficacy and minimize adverse effects(Bruni et al., 2017; Huang et al., 2021).

Among possible cell targets, podocytes have become a focus in recent years as a key target in renal diseases (Bruni et al., 2017; Cellesi et al., 2015; Colombo et al., 2017). These highly specialized polarized cells of

the glomerular filtration barrier (GFB)(Cellesi et al., 2015) are particularly susceptible to various biological stresses, including genetic mutations, as well as inflammation, toxicity, metabolic imbalances, and altered hemodynamics(Barutta et al., 2022; Cellesi et al., 2015). Their damage leads to structural (foot process retraction and cell detachment) and functional (increased protein leakage though GFB) derangements (Cellesi et al., 2015).

Recent studies demonstrated that the neurotrophin Brain Derived Neurotropic Factor (BDNF) has restorative effects on podocyte cyto-skeleton damage in vitro and in vivo(Li et al., 2015) Upon binding to its

receptor tropomyosin-related kinase-B (TrkB), also expressed by this cell type(Géral et al., 2013; Li et al., 2015), BDNF stimulates actin polymerization by activation of the kinase Limk1 and cofilin phosphorylation resulting in improved podocyte structure and reduced protein loss (Li et al., 2015). These findings constitute the basis for a possible treatment of chronic kidney diseases(Badeński et al., 2022; Gao et al., 2022; Lee et al., 2015; Leeuwis et al., 2010; Ozkan et al., 2022). Since BDNF is a promising biotherapeutics for treating neurological disorders (Géral et al., 2013), its safety has been established through human trials, although its efficacy is limited by its short half-life in blood circulation (Géral et al., 2013), and the applicability of BDNF is also hindered by the expression of TrkB by multiple cell types(Andreska et al., 2020; Cardenas-Aguayo et al., 2013; Géral et al., 2013; Kraemer et al., 2005). To maximize its therapeutic potential, it is essential to develop biocompatible nanocarriers that can selectively deliver BDNF to the target cells while protecting it from rapid clearance in the bloodstream.

Recent advancements in nanomedicine and drug delivery have led to the development of new nano-based therapeutics for treating various kidney diseases, such as kidney cancer(Kulkarni et al., 2016; Liu et al., 2015; Singh et al., 1989), acute kidney injury, and chronic kidney disease(Huang et al., 2021; Scindia et al., 2008; Suana et al., 2011; Wang et al., 2020; Zhou et al., 2021) (Oroojalian et al., 2020). Despite the remarkable promise, their efficacy is limited by biological barriers encountered in the blood circulation and at the kidney target sites.

Liposomes are a widely recognized nanodelivery system with significant clinical acceptance. They consist of biocompatible vesicles composed of at least one phospholipid bilayer that envelops an aqueous core[27, 28]. When decorated with polyethylene glycol (PEG), liposomes significantly reduce the risk of opsonization and clearance by the mononuclear phagocytic system during blood circulation(Hwang et al., 2012; Immordino et al., 2006; Pattni et al., 2015). Additionally, liposomes can be easily modified with ligands, such as antibodies or homing peptides, for improved targeting. By encapsulating hydrophilic drugs specific for podocytes and targeting them to the glomerulus, exposure to undesirable substances in vivo can be avoided.

Recently, PEGylated low temperature sensitive liposomal formulations have been optimized to encapsulate a range of payloads, including large macromolecules and proteins, such as BDNF, while preserving their activity in vitro(Huang et al., 2017). Low temperature sensitive liposomes (LTSL) offer key benefits compared to traditional liposomes. Their relatively low gel-liquid crystal transition temperature (Tm) enables protein encapsulation under mild conditions, which is often crucial for avoiding protein denaturation(Xu et al., 2012). Moreover, these liposomes may also be used for triggered drug delivery to cells, tissues, and organs, through the use of local hyperthermia(Chaudhry et al., 2022; Ta and Porter, 2013) or high-intensity focused ultrasound (Gasselhuber et al., 2012; Zhan et al., 2019). In fact, at body temperature the lipid membrane has low permeability for hydrophilic compounds, while above the Tm, when the targeted area is exposed to a local increase in temperature, the drug is released, either by increasing the permeability of the membrane or by causing its rupture(Chaudhry et al., 2022; Ta and Porter, 2013).

When selecting liposomal nanocarriers for targeted podocyte delivery, it is important to consider the size limitations imposed by the kidney filtration barrier. This barrier, which is composed of the glomerular endothelium, the glomerular basement membrane, and podocyte filtration slits, has a maximum effective size cutoff of 5–10 nm for the entry of molecules and particles into the urinary space(Bruni et al., 2017). As a result, intact liposome-based nanocarriers are unlikely to cross this barrier to reach the podocytes. However, by designing the nanocarriers to release their payload in close proximity to the podocyte layer, the therapeutic molecules can be effectively delivered to their intended target.

In this study, we aimed to design LTSL for the encapsulation and targeted delivery of BDNF to podocytes, while maintaining stability and biological activity, and exploiting the conjugation of targeting peptides to enhance the therapeutic effect in vitro (Fig. 1).

While cyclic RGD (cRGD) can be selected for targeting endothelial cells in preliminary in vitro assessment, a more targeted peptide specific to kidney glomeruli is necessary to achieve in vivo translation. The peptidic sequence HITSLLS (abbreviated as HIT) was previously identified to home to the endothelial glomeruli using in vivo phage display (Denby et al., 2007; Denby et al., 2006; Gray and Brown, 2014). This peptide was therefore selected and modified with a terminal cysteine (HITSLLSC) to be conjugated to the distal end of the maleimide-functionalized PEGylated phospholipids of liposomes through Michael type addition. The nanosystems were assessed in vitro on podocyte and endothelial cell cultures, and via a podocyte-endothelial cell co-culture device as a GFB model. Preliminary in vivo evaluations were finally conducted to assess the effectiveness of the nanoformulation on murine glomeruli repair and identify potential obstacles for its future translation as a promising strategy for treating glomerular diseases.

2. Materials and methods

2.1. Materials

1,2-dipalmitoyl-*sn*-glycero-3-phosphocholine (DPPC), 1-palmitoyl-2-hydroxy-*sn*-glycero-3-phosphocholine (P-Lyso-PC), Cholesterol (Chol), (1,2-distearoyl-*sn*-glycero-3-phosphoethanolamine-N-[methoxy (polyethyleneglycol)-2000] (DSPE-PEG2000), 1,2-dipalmitoyl-*sn*-glycero-3-phosphoethanolamine-N-(lissamine rhodamine B sulfonyl) (Rhod-DPPE), 1,2-distearoyl-*sn*-glycero-3-phosphoethanola-mine-N-maleimide (polyethylene glycol) (DSPE-PEG2000-Mal) were purchased from Avanti Polar Lipids (Alabaster, US). Albumin-fluorescein isothiocyanate conjugate (FITC-albumin), fluorescein isothiocyanate isomer I (FITC, ≥90 % (HPLC)), bovine serum albumin (BSA), tris(2-carboxyethyl) phosphine (TCEP, immobilized on Agarose CL-4B), Adriamycin (ADR), collagenase II and IV, Paraformaldehyde (PAF) were purchased from Sigma-Aldrich (Milan, Italy). HBS was purchased from Euroclone S.p.a, Italy, Milano. vWF antibody was purchased from DAKO Agilent Technologies Singapore (International) Pte Lt and secondary AlexaFluor 488 donkey anti rabbit from Invitrogen- Thermo Fisher Scientific (MA USA).

Brain-derived neurotrophic factor (BDNF, human recombinant) was obtained from QED Bioscience Inc. (Histo Line, Milano, Italy). RGD-(D-Phe)-C (cRGD), Ac-HITSLLSC-NH2 (HIT) were synthesized by CASLO ApS (Lyngby, Denmark).

2.2. Preparation of BDNF-loaded liposomes

Liposomes [(LTSL: DPPC/P-Lyso-PC/DSPE-PEG2000 = 90/10/4 (mol/mol)] were prepared by the lipid film hydration and extrusion method. Respective lipids (total lipids content was 10 µmol) were dissolved in dichloromethane/methanol mixed solutions (V/V = 9/1) in a round-bottomed flask, and the solvent was evaporated under vacuum in a rotary evaporator until a thin lipid film was formed. Then 100 µg of BDNF dissolved in 0.5 ml PBS buffer (10 mM, pH = 7.4) was used to hydrate the lipid film at 50 °C to obtain a lipid concentration of 20 mM. Afterward, the suspension of multilamellar vesicles (total lipid concentration 20 mM) were subjected to 6 freeze–thaw cycles and sized by repeated extrusion (Avanti extruder) through polycarbonate membranes (pore size 0.1 µm) to obtain unilamellar liposomes. Free BDNF was separated from BDNF-loaded liposomes (BDNF-LTSL) by gel filtration chromatography through a Sepharose CL-4B column (Sigma-Aldrich, Milan, Italy). When fluorescent nanocarriers were needed for in vitro/in vivo tests, liposomes were labelled with 0.2 mol% of rhodamine through the inclusion of Rhod-DPPE.

2.2.1. Loading and encapsulation efficiency

2 µL of Triton-X100 (10 %, v/v) was added to 50 µl of BDNF-LTSL to disrupt the liposome compartments, incubated for 30 min, and diluted in PBS buffer to a total volume of 100 µL. The concentration of BDNF was
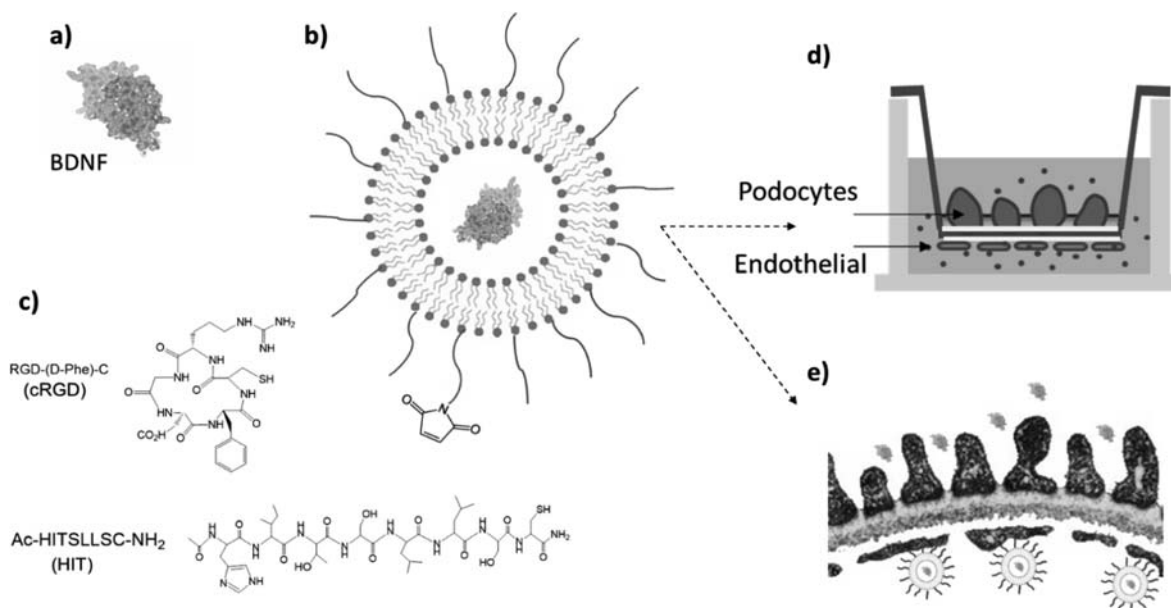
Fig. 1. BDNF proteins (a) are encapsulated in LTSL (b), which are further functionalized with targeting peptides (c). The nanosystem was assessed in vitro via a podocyte-endothelial cell co-culture device as GFB model (d) and in vivo to evaluate accumulation and releases on murine glomeruli (e).

determined through BDNF Elisa Kit Assay (Abcam, Milan, Italy) according to the manufacturer's protocol. Encapsulation efficiency (EE) and loading efficiency (LE) were calculated as follows:

$$LE(\%) = \frac{total \mu mol of payload trapped in liposomes}{total \mu mol of lipids} \times 100 \quad (1)$$

$$EE(\%) = \frac{total amount of payload trapped in liposomes}{total amount of payload added} \times 100 \quad (2)$$

2.2.2. Dynamic light scattering (DLS) analysis

Liposomal formulations were diluted to 0.5 mM with PBS buffer (10 mM, pH = 7.4) and the average particle size and size distribution were measured by DLS via a Zetasizer Nano ZS (Malvern Instruments Ltd., UK) equipped with a 4 mW helium/neon laser at a wavelength output of 633 nm and a backscattering angle of 173° at 25 °C.

2.2.3. Sds-polyacrylamide gel electrophoresis (SDS-PAGE)

SDS-PAGE analysis was carried out on samples where the protein amount per band was standardized to 2–5 μg. Electrophoresis was run in a constant current mode at 200 V on discontinuous stacking (5 %) and separating gels (15 %). Gels were stained by Brilliant blue R (Sigma) solution (0.1 % Brilliant Blue R, 25 % ethanol, 8 % acetic acid.).

2.2.4. Peptide conjugation

Firstly, LTSL was modified with maleimide functional groups by incorporating 2 mol % of DSPE-PEG2000-Mal to the liposomal formulation [DPPC/P-Lyso-PC/DSPE-PEG2000/DSPE-PEG2000-Mal = 90/10/2/2 (mol/mol)]. Maleimide bearing LTSL encapsulated with BDNF (BDNF-LTSL-Mal) were prepared by the lipid film hydration method as described previously. Then cRGD or HIT peptide (1 mg/ml) was pretreated with TCEP immobilized on Agarose CL-4B to reduce the existing disulfide bonds according to the protocol provided by the manufacturer, and 12 μL peptide solution [peptide/maleimide (mol/mol) = 1/10] was added into the aqueous solution of BDNF-LTSL-Mal and the reaction was carried out at 4 °C for 24 h. Excess amount of unbound peptide was removed by gel filtration through a Sepharose CL-4B column and the peptide-conjugated BDNF-LTSL suspension (BDNF-LTSL-cRGD or BDNF-LTSL-HIT) was obtained.

2.3. In vitro assessment

2.3.1. Cell cultures

The mouse microvascular endothelial cell line (EOMA) was obtained from ATCC (ATCC number: CRL-2586, LGC Standards S.r.l., Sesto San Giovanni, Milan, Italy) and used as a capillary endothelium model. As indicated by the ATCC protocol, cells were grown in DMEM/F12 supplemented with 10 % FBS, 100 U/ml penicillin, 100 mg/ml streptomycin, 4 mM L-glutamine.

The conditionally immortalized mouse podocytes (SV1) were obtained from CLS (CLS Cell Line Service Ltd, Eppelheim, Germany). Cells were cultured at 33 °C in DMEM/F-12 containing 10 % of FBS, 100U/ml penicillin, 100 mg/ml streptomycin, 2 mM L-glutamine and 20 U/ml recombinant mouse gamma-interferon (γ-IFN) for proliferation. To initiate the differentiation, cells were thermo-shifted to 37 °C and maintained in medium (DMEM-F12, supplemented with 10 % FBS, 5 mg/ml transferrin, 10^{-7} M hydrocortisone, 5 ng/ml sodium selenite, 0.12 U/ml insulin, 100 U/ml penicillin, 100 mg/ml streptomycin, 2 mM L-glutamine) without γ-IFN.

2.3.2. Fluorescence microscopy

SV1 podocytes were seeded on cover slips in 6 well plates with a seeding density of 2×10^4/wells and culture at 37 °C in completed medium without γ-interferon for 3–4 days. Cells were incubated with 0.8 μM ADR for 24 h to cause damage of the cells. Then free BDNF and or BDNF-LTSL (200 ng/ml) were added to the cells and incubated for 48 h.

Phalloidine staining of the podocyte cytoskeleton was obtained by fixing the cells with 4 % paraformaldehyde for 10 min and then permeabilized with 0.3 % Triton X-100. Afterwards, cells were incubated with 1 % of BSA for 30 min at room temperature (RT) to block any unspecific recognition. Then a mixed solution of Phalloidin-FITC (Sigma-Aldrich) at 1:100 dilution and DAPI at 1:1000 dilution was added and further incubated for 1 h at RT. After 1 h incubation, the mixed solution was removed, and the cells were washed thoroughly with PBS several times and mounted. Images were acquired by Zeiss AxioObserver microscope equipped with high resolution digital videocamera (AxioCam, Zeiss) and Apotome system for structured illumination, and recorded by AxioVision software 4.8.

For the evaluation of EOMA-liposome interaction, EOMA cells were grown on cover slips in 6 well plates with a seeding density of 2×10^5/

wells for 24 h. Then liposome samples were diluted to 0.5 mg/ml with cell culture medium and incubated with the cells for 24 h. Afterwards, cells were washed with PBS and nuclei were stained with DAPI, and observed by fluorescence microscopy as described above.

2.3.3. Cell co-culture system and BSA permeability assay

The podocyte-endothelial cell co-cultures were assembled as described by Li et al.(Li et al., 2016). Briefly, using the Millicell hanging cell culture inserts with Polyethylene Terephthalate (PET) microporous (1 μm diameter) membrane (Millipore, Milan, Italy) coated on both sides with collagen type IV (Sigma Aldrich, Milan, Italy), 1.5×10^5 of EOMA cells were seeded on the lower side of the membrane and allowed to adhere to it for 4 h. EOMA cells were cultured in medium containing 5 ng/ml of VEGF for one week before 6.5×10^4 podocytes were seeded on the upper side of the membrane and covered by their own medium. Podocytes and endothelial cells were co-cultured in their respective medium for another one week before experiments. In order to assess albumin permeability, cells were carefully washed on both sides with PBS. Then, the upper (podocyte) compartment was filled by DMEM/F-12 and the lower (endothelial) compartment was filled by DMEM/F12 supplemented with 40 mg/ml BSA. Medium was taken from the upper compartment after 2 h incubation and albumin content was measured and taken as the basal level (BSAb). After treatment of the co-culture with the desired substances, the BSA content was analysed again as before (BSAexp), and the results were expressed as: (BSAexp-BSAb) / BSAb x 100 %. BSA concentration was measured by spectrometry using the DC protein assay kit (Bio-Rad, Milano, Italy).

After performing the basic BSA permeability test at standard culture condition, ADR was added to the podocyte compartment at a concentration of 0.8 μM and is incubated for 24 h. Afterwards, the co-culture inserts were washed with PBS, the medium was replaced by fresh medium to remove ADR completely, and the permeability of BSA was re-evaluated repeating the same steps above. Then BDNF-LTSL or BDNF-LTSL-cRGD (equivalent to 200 ng/ml BDNF in cell culture medium) was added to the upper (Podocyte) compartment or lower (endothelial cell) compartment and incubated for 24 and 48 h. Free BDNF and medium alone were used as controls. At the end of 24–48 h incubation, the BSA permeability tests were performed as previously described.

The liposomal permeability was also calculated as percent of the concentration of fluorescent liposomes recorded in the upper compartment at 24 and 48 h with respect to the initial concentration in the lower compartment, and it was evaluated by measuring the fluorescence intensity (SAFAS Flx-Xenius, Monaco, France) of the medium removed from the upper and lower compartments, respectively.

To simulate hyperthermia conditions and achieve thermoresponsive release of the payload, liposome suspensions were pre-heated at 42 °C for 30 min and then incubated with the co-culture system at physiological temperature (37 °C) as described above.

2.3.4. Rat glomerular endothelial cell (rGECs)

Glomeruli were isolated from renal cortex of 7 week-old Sprague Dawley rats, by standard sieving technique in Hank's Balanced Salts Solution (HBSS). Glomeruli were re-suspended in a solution of collagenase II and IV for 15 min at 37 °C. The digestion was then blocked by adding 5 % FBS in HBSS and the cell suspension was centrifuged. The pellet was then treated with trypsin diluted in HBSS for further 15 min at 37 °C and, after blocking the trypsin activity with 5 % FBS, the cell suspension was passed through a 100 μm mesh. After centrifugation the cells were plated on fibronectin coated flask in endothelial cell medium (Invitrogen). Characterization of isolated cells was performed by immunofluorescence analysis of von Willebrand factor (vWF), a marker for endothelial cells. After fixation (PAF 1 % in PBS w/o calcium and magnesium) and permeabilization (0,1% Triton), vWF was detected by rabbit anti vWF antibody (1:20 Dako) and secondary anti rabbit antibody. Nuclei were stained with DAPI. Images were acquired by microscope Leica DM 2000 equipped with Leica DFC490 camera. As negative

control unrelated Dako was used.

Liposomes-rGECs interaction was evaluated by incubation of Cells cultured on the fibronectin coated poly-D-lysine cellware (Corning) with liposomes (0.5 mg/ml) for 24 h. After that the cells were washed with PBS w/o calcium and magnesium and fixed with 1 % PAF. Nuclei were stained with DAPI. Images were acquired by microscope Leica DM 2000 equipped with Leica DFC490 camera.

2.4. In vivo assessment

2.4.1. Biodistribution of liposomes in mice

To evaluate the biodistribution of liposomes-peptides after intravenous injection, 8 ~ 10 week old male BALB/C mice (Envigo Rms Srl, San Pietro al Natisone, UD, Italy) and Adriamycin nephropathy (ADRN) mice were tested. ADRN was induced by a single injection of 10 mg/kg ADR in the tail vein. Urinary albumin was monitored every other day by Albustix (Bayer, Milan, Italy). After one week of ADR administration, mice with evident proteinuria (3–4 +), as well as healthy mice, were randomized (3 mice/group) to receive different rhodamine-labeled HIT-LTSL at dosage of 0.5 mg of lipids intravenously (injected volume 200 μl) via tail vein. Mice were sacrificed after 2 h from injection, and liver, spleen, lung and kidney were removed, embedded in optimum cutting temperature cryoembedding matrix (OCT, Tissue-Tek, Società Italiana Chimici, Roma, Italy), snap-frozen in a mixture of isopentane and dry ice and stored at –80 °C. Mice which received only physiological solution, and rhodamine-labeled LTSL without HIT functionalization, were used as control.

For fluorescence microscopy observation, 5-μm-thick tissue cryosections were fixed with 4 % of paraformaldehyde at room temperature for 10 min. Nuclei were stained with DAPI at concentration of 0.1 mg/ml in PBS for 30 min. Slides were mounted with Fluorsave aqueous mounting medium (Calbiochem, VWR International, Milan, Italy). Images were acquired and recorded as previously described. The percentage of the Rhodamine positivity area from 10 images of each sample were analysed by Image J software.

2.4.2. Treatment of Adriamycin nephropathy mice with BDNF-LTSL-HIT

ADRN was induced as previously described. 8 days after ADR injection, mice with 3–4 + proteinuria (Albustix test) were randomized to receive vehicle (0.9 % NaCl), LTSL-HIT, BDNF, BDNF-LTSL-HIT, 20 μg/day from day 8 to day 10 (5 mice/group) for a total dosage of 60 μg BDNF /mouse. Mice were sacrificed on day 14. Urine was collected both before and 7 days after ADR injection, as well as before sacrifice and the kidneys were removed for histology examination. Urinary albumin was analysed using mouse albumin ELISA Kit (Bethyl Laboratories, Montgomery, TX, USA) and urinary creatinine assay was performed using urinary creatinine assay kit (Cell Biolabs Inc, San Diego, CA, USA) as manual instruction.

2.4.3. Ethical approval

A total of 131 Male BALB/C mice, age 8–10 weeks, average body weight 25 ± 1.4 g, were obtained from ENVIGO RMS Srl (Udine, Italy) and maintained in the Stabilimento di Scienze Chirurgiche, Fondazione IRCCS Ca' Granda Ospedale Maggiore Policlinico, Milano. The animals were fed a normal chow diet and water and housed under standard conditions with a controlled temperature (~22 °C) and humidity (~60 %) and were exposed to a 12/12-h light dark cycle. Animal protocols strictly adhered to the Public Health Service Policy on Humane Care and Use of Laboratory Animals (D.L.116–27/01/1992) and were approved by the organization responsible for welfare of animals of Milan university and by the Italian Ministry of Health (authorization N. 1058/2016 PR, 550/2019 PR).

The protocols for isolation of rodent glomeruli and primary cells were approved by the Ethics Committee for Animal Experimentation (OPBA) of the University of Trieste (no PO1640ZEN1) in compliance with the Italian regulation (D.L.vo 26/2014) and the Directive 2010/63/

EU of the European Parliament.

2.5. Statistics

The data were presented as mean ± standard deviation of three different replicates and analyzed for statistical significance by Student's two-tailed *t*-test and ANOVA (assuming equal variance).

3. Results

3.1. Preparation of BDNF-loaded liposomes

BDNF was successfully encapsulated in PEGylated low temperature sensitive liposomes (Fig. 1) by the lipid film hydration and extrusion method(Huang et al., 2017). The LTSL formulation (DPPC/P-Lyso-PC/DSPE-PEG2000 = 90/10/4) allowed to encapsulate BDNF at mild temperature (50 °C), obtaining a loading efficiency LE of 4 mmol/mol% and the encapsulation efficiency EE of 12 %. According to DLS analysis, BDNF-LTSL formulation presented an average particle size of 152 ± 2 nm, and during storage at 4 °C, this colloidal suspension maintained a constant particle for at least one month. (Fig. 2A). The stability and the activity of BDNF was assessed both before (supporting info, Figure S1) and after liposomal encapsulation. Since the presence of sodium dodecyl sulfate in the SDS-PAGE system (Fig. 2B) leads to the rupture of the lipid vesicles, BDNF was released and analyzed by gel electrophoresis without previous separation. Results showed that loaded BDNF displayed the same band as that of original BDNF, even after being preheated at 42 °C for 30 min and further incubated at 37 °C for 24 h.

3.1.1. Peptide conjugation

Cyclic RGD (cRGD) was selected as homing peptide for in vitro tests, due to its availability and well-known capability of targeting endothelial cells, via αvβ3 integrin binding(Amin et al., 2015; Danhier et al., 2012; Song et al., 2017). The presence of a thiol cysteine residue enables cRGD to be linked to maleimide bearing liposomes using sulfhydryl–maleimide coupling chemistry(Koning et al., 2004; Oswald et al., 2016). The conjugation reaction was optimized via HPLC analysis to maximize the conversion and to select the optimal grafting density to achieve adequate adhesion to endothelial (EOMA) cell cultures (supporting info). The results indicated that at least 0.2 mol% of cRGD should be grafted to liposomes to achieve enhanced cellular adhesion and uptake of LTSL-cRGD.

Since cRGD presents low specificity towards the endothelial cells of the glomerular capillaries(Janssen et al., 2002), the HIT peptide was selected for homing to the endothelial glomeruli(Denby et al., 2007; Denby et al., 2006; Gray and Brown, 2014), and modified with a terminal cysteine (HITSLLSC) to be conjugated to the liposomes through Michael type addition, as used for cRGD conjugation. Physicochemical characterisation of HIT conjugated liposomes (LTSL-HIT) via HPLC confirmed the quantitative peptide functionalization (supporting info). Tests also confirmed that the particle size distribution of LTSL was not affected by the conjugation of the peptides (supporting info, Figure S4).

3.2. In vitro assessment

3.2.1. Biological activity of BDNF-LTSL

The biological activity of BDNF-LTSL was investigated by observing the F-actin cytoskeleton of podocytes in vitro. Normal cells displayed substantial F-actin fibers with regular distribution along whole cell body and processes (Fig. 3A a). However, the F-actin fibers appeared irregular and cortical distribution when podocytes were treated with ADR, indicating a significant podocyte damage (Fig. 3A b). 48 h incubation with free BDNF (Fig. 3A c) as well as BDNF-LTSL (Fig. 3A d) led to cytoskeleton repair, as demonstrated by the increase of F-actin fiber density with more regular distribution.

The bioactivity of BDNF-LTSL was also evaluated through a BSA permeability assay, based on a podocyte-endothelial cell co-culture device(Li et al., 2020; Li et al., 2016) which was specifically developed to mimic the GFB in vivo (Fig. 1d). The presence of a permeable membrane between the podocyte and the endothelial cell layers allowed to perform a functional assessment of this GFB-mimicking barrier. A pre-treatment of the co-culture with ADR for 24 h led to an abundant increase of albumin permeability, as an effect of induced cell damage (Fig. 3B–C). When BDNF-LTSL were added into the podocyte (upper) compartment for 24 h, the BSA permeability clearly decreased, as compared to the effect of simple cell culture medium, although this effect was less pronounced than that obtained with the addition of free BDNF (Fig. 3B). When the incubation time was extended to 48 h, the permeability of BSA was markedly reduced below the control values, and the effect of BDNF-LTSL was comparable to that of free BDNF. This result may be attributed to the trophic activity of BDNF on podocyte cell processes (Li et al., 2015), which not only recovers the podocyte cytoskeleton damaged by ADR but also ameliorates their structure compared to cells cultured in medium without BDNF. The effect of adding the liposomes to the endothelial (lower) compartment was also investigated (Fig. 3C). In this case, BDNF-LTSL was still able to decrease BSA permeability, although
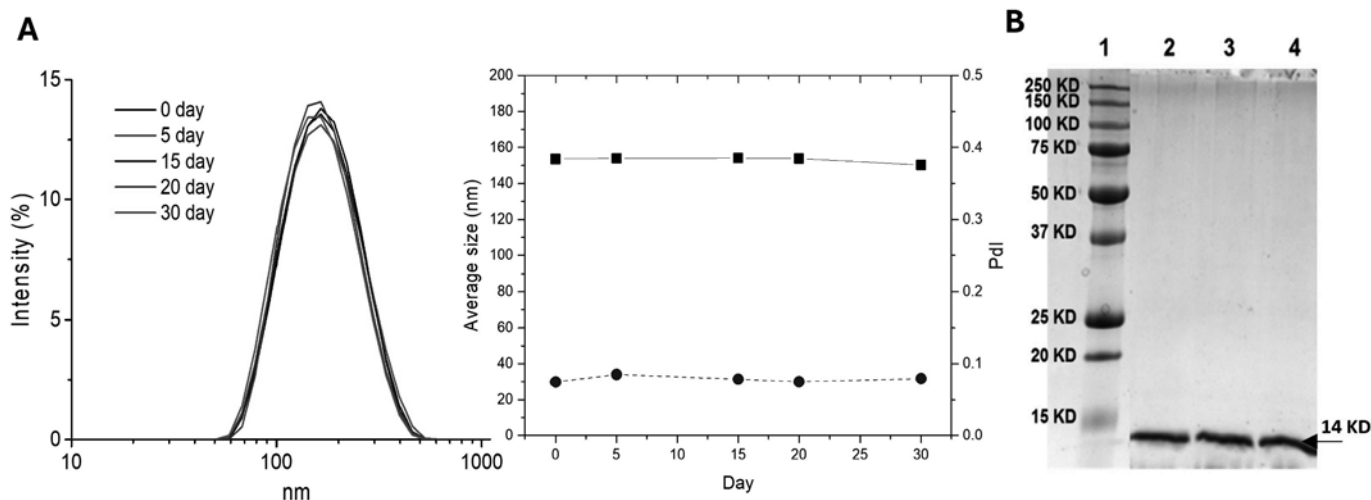

Fig. 2. A) Size distribution curves, Z-average size, and polydispersity index (PdI) of BDNF-LTSL stored at 4 °C as measured by DLS at different days. B) SDS-PAGE of BDNF-loaded LTSL liposomes at different conditions: Lane 1: standard; Lane 2: BDNF-LTSL; Lane 3: BDNF-LTSL after being incubated at 37 °C for 24 h; Lane 4: BDNF-LTSL after being preheated at 42 °C for 30 min and further incubated at 37 °C for 24 h.
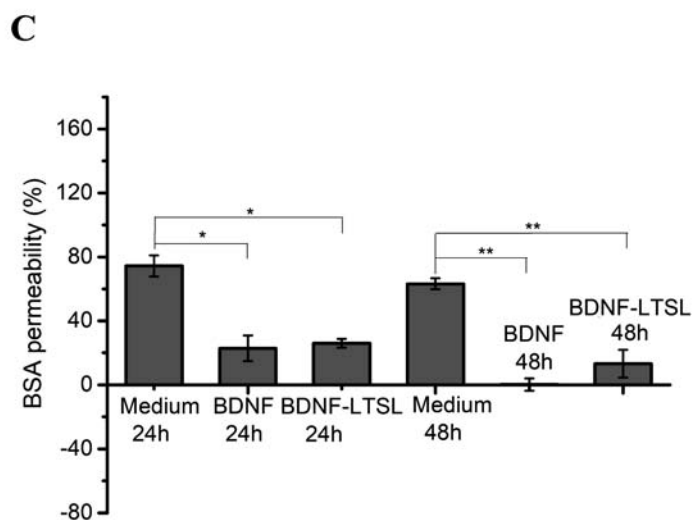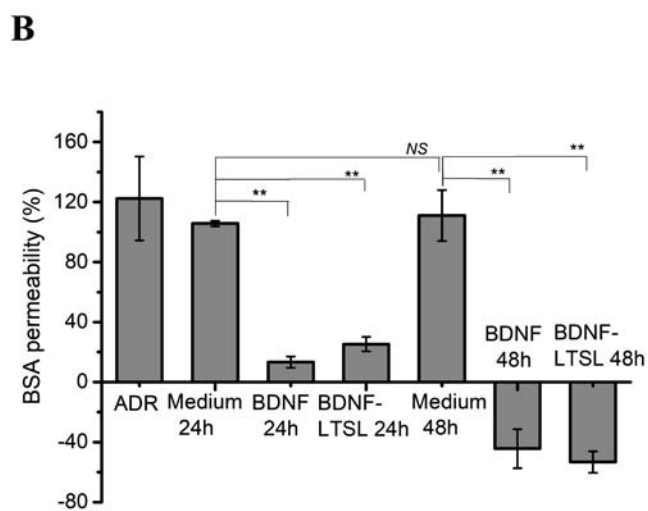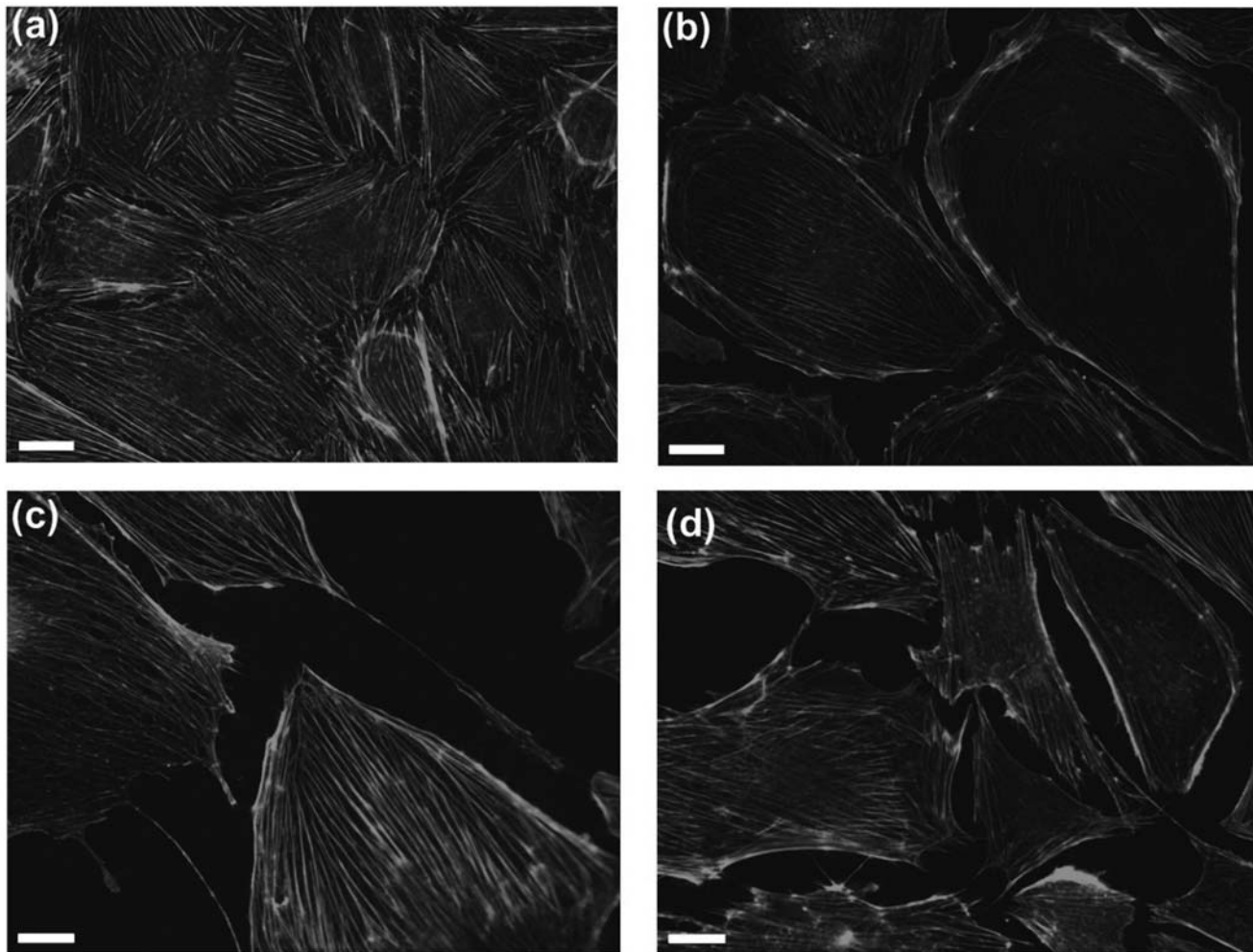
Fig. 3. A) Morphology of podocytes stained by phalloidin. (a) Normal cells; (b) cells after ADR treatment; (c) cells after ADR treatment and incubated with free BDNF; (d) cells after ADR treatment and incubated with BDNF-LTSL (200 ng/ml BDNF in 0.2 mg/ml lipids) for 48 h. scale bar: 20 μm. B) Percent increase of BSA permeability when samples were added to the upper (podocyte) compartment of the podocyte-endothelial cell co-culture device; C) Percent increase of BSA permeability when samples were added to the lower (endothelial) compartment; cell co-culture was pre-treated with ADR, then incubated for 24 h and 48 h with culture medium, 200 ng/ml of BDNF, or BDNF-LTSL (equivalent to 200 ng/ml BDNF) (n = 3, *p < 0.05 and **p < 0.01, NS not significant).

this response was reduced when compared to the direct administration to the podocyte compartment. The difference was particularly evident after 48 h incubation, which may be ascribed to the lack of permeation of liposomes to the upper compartment, and possibly to a partial BDNF uptake by the endothelial cells once the protein was released by the lipid vesicles.

In the absence of co-culture damage, when the cells were kept for 24 h without ADR before treatment, the effect of BDNF and BDNF-LTSL was very limited. In fact, BSA permeability increased by less than 5 % when the co-culture was incubated for 24 h with medium, decreased by 15 % only when BDNF or BDNF-LTSL were added to the upper (podocyte) compartment, and changed within 6 % when they were added to the lower (endothelial) compartment (supporting info, Figure S6).

3.2.2. Biological activity of BDNF-LTSL-cRGD

BDNF encapsulated in LTSL-cRGD liposomes (BDNF-LTSL-cRGD) was still active and able to repair podocytes in vitro, similarly to what

was obtained with unconjugated liposomes (supporting info, Figure S5). The repairing effect on BDNF-LTSL-cRGD on GFB damage was also assessed using the co-culture in vitro model. The liposomes were too large (hydrodynamic diameter ∼ 150 nm) to cross the co-culture filter, as confirmed by their very limited permeation after 24 h (<2%) and 48 h (<4%) (Fig. 4A), therefore it was assumed that only free BDNF can pass through the GFB and exert its repairing effects on podocytes. BDNF delivery and permeation across the co-culture filter were achieved by pre-heating BDNF-LTSL-cRGD at 42 °C for 30 min, which allowed the thermoresponsive release of the payload, as previously reported (Huang et al., 2017). Under this condition, the BSA permeability after ADR damage was abundantly reduced when the formulation was added to the lower (endothelial) compartment and incubated for 48 h, while without pre-heating, its effect was almost negligible (Fig. 4B). This may be due to the internalization of BDNF-LTSL-cRGD by endothelial cells, possibly followed by endosomal degradation. To verify this hypothesis, we stained the endothelial cell layer of the co-culture with phalloidin-FITC
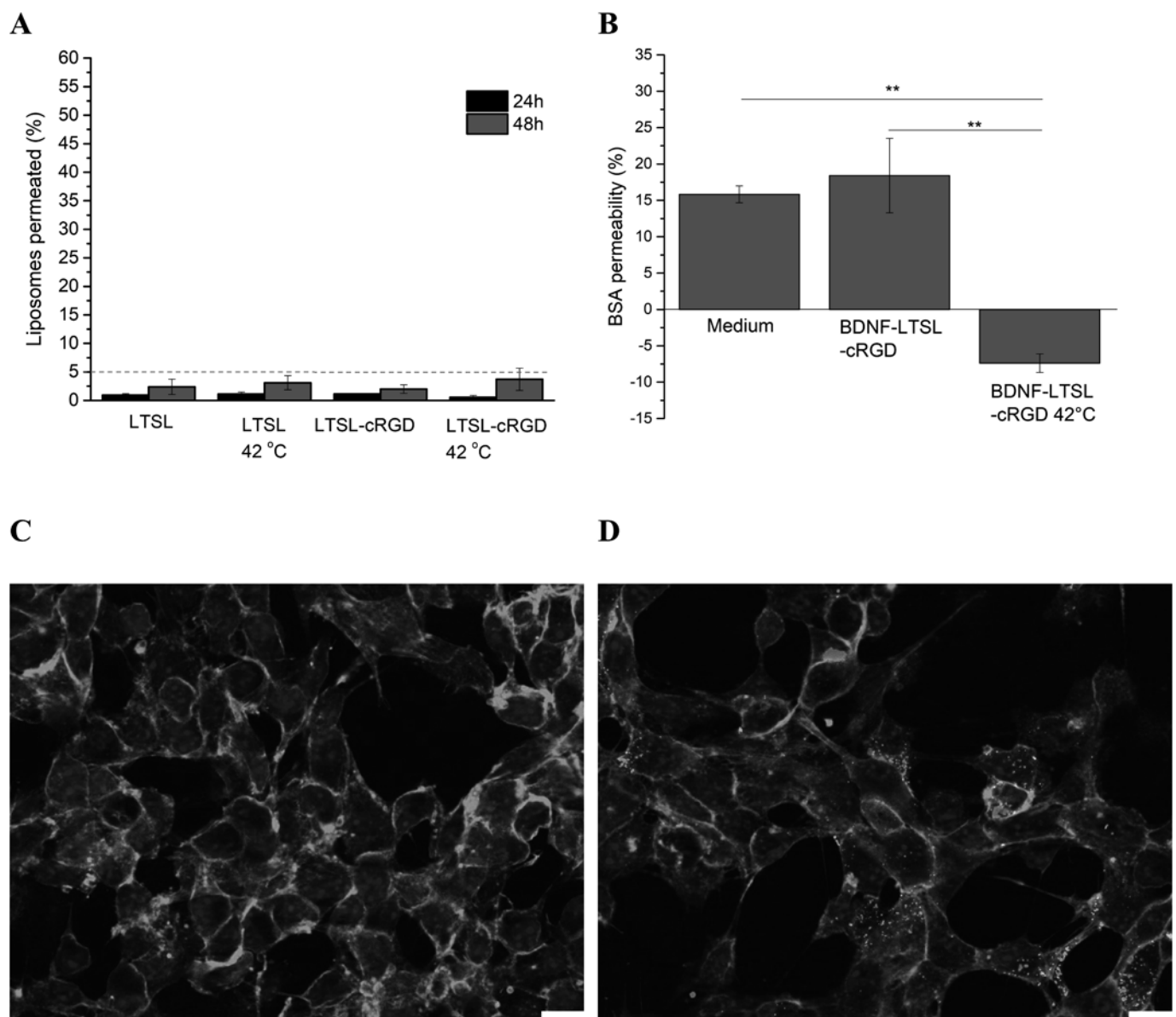

Fig. 4. A) Percent of BDNF-loaded liposomes permeated through the co-culture filter at 24 and 48 h. B) BSA permeability when samples were added to the lower (endothelial) compartment, with/without pre-heating at 42 °C (n = 3, *p < 0.05 and **p < 0.01) and incubated for 48 h. Cellular uptake of BNDF-LTSL (C) and BNDF-LTSL-cRGD (D) liposomes by EOMA cells in the co-culture filter after 48 h incubation. Phalloidine-FITC (green), DAPI (blue), Rhodamine-labeled Liposomes (red). Scale bar 20 μm. (For interpretation of the references to colour in this figure legend, the reader is referred to the web version of this article.)

after incubation with rhodamine-labelled BDNF-LTSL-cRGD for 48 h. BDNF-LTSL-cRGD presented significant uptake (Fig. 4C–D) while without cRGD peptide, no liposome-cell colocalization was noticed.

3.2.3. Bioactivity of BDNF-LTSL-HIT

When EOMA cells were incubated for 24 h, the fluorescent signal of Rhodamine-labeled LTSL-HIT was insignificant compared to that of LTSL-cRGD (Fig. 5A), suggesting that the interaction of EOMA cells with LTSL-HIT was negligible, as expected. On the other hand, rat glomerular endothelial cells (rGECs) were utilized as a model to verify the interaction between LTSL-HIT and the glomerular endothelial cells, which reflects the in vivo target. The successful isolation of rGECs from rats was confirmed by immunofluorescence staining with anti-von Willebrand factor (vWF) which is specifically expressed on endothelial cells(Jahroudi and Lynch, 1994) (supporting info, Figure S7). The cellular uptake tests clearly showed that LTSL-HIT displayed significant uptake by rGECs, while the ligand-free PEGylated liposomes, i.e., LTSL, did not, thus confirming the specific interaction between the peptide-conjugated liposomes and rGECs (Fig. 5B).

3.3. In vivo assessment

3.3.1. Biodistribution of liposomes in mice

Biodistribution of HIT- conjugated liposomes was studied in healthy mice as well as in ADRN mice. After intravenous injection, both healthy and ADRN mice presented a major sequestration of LTSL-HIT by the liver, followed by the spleen (Fig. 6A), in agreement with typical clearance effect of the Mononuclear Phagocyte System (MPS) on peptide-functionalised liposomes (Allen et al., 1995; Kelly et al., 2011; Lucas et al., 2017). Although modest, the presence of liposomes in the

kidney was more evident than in lungs, as a possible effect of HIT peptide targeting. The quantitative analysis of the fluorescence microscopy images confirmed this observation (Fig. 6B–C), with the highest percentage of rhodamine-positive area in the liver, followed by the spleen, and with more deposition of LTSL-HIT in kidney than in lungs. On the other hand, the biodistribution of non-functionalized LTSL showed negligible accumulation in the kidneys of both healthy and ADRN mice (supporting info., Figure S8).

3.3.2. Treatment of ADR nephropathy with BDNF-LTSL-HIT

To verify if encapsulation of BDNF into HIT-conjugated liposomes can provide a therapeutic effect, we used minor dosage (60 μg BDNF per mouse) compared with our previous study (1 mg/mouse(Li et al., 2015)) to treat ADRN. 8 days after ADR injection, mice were randomized to receive vehicle (0.9 % NaCl), LTSL-HIT, free BDNF, and BDNF-LTSL-HIT, from day 8 to day 10 for a total dosage of 60 μg BDNF /mouse, and finally sacrificed on day 14. As showed in Fig. 7, free BDNF and empty LTSL-HIT were not able to reduce proteinuria at day 14, whereas the BDNF-LTSL-HIT demonstrated a small but detectable decrease of the urinary albumine/creatinine ratio. The positive but limited effect of the treatment is compatible with the relatively low amount of liposomal accumulation in the kidney glomeruli, as confirmed by the biodistribution tests.

Histological examination of the kidney tissue with hematoxylin-eosin staining (Fig. 8), revealed focal and segmental glomerular damage, numerous dilated tubules, and evident tubular protein casts, in mice treated with vehicle (0.9 % NaCl). LTSL-HIT and free BDNF treatment did not change the histological characteristics compared with vehicle treatment, While BDNF encapsulated in LTSL-HIT ameliorated kidney damage, which was highlighted by the disappearance of tubular
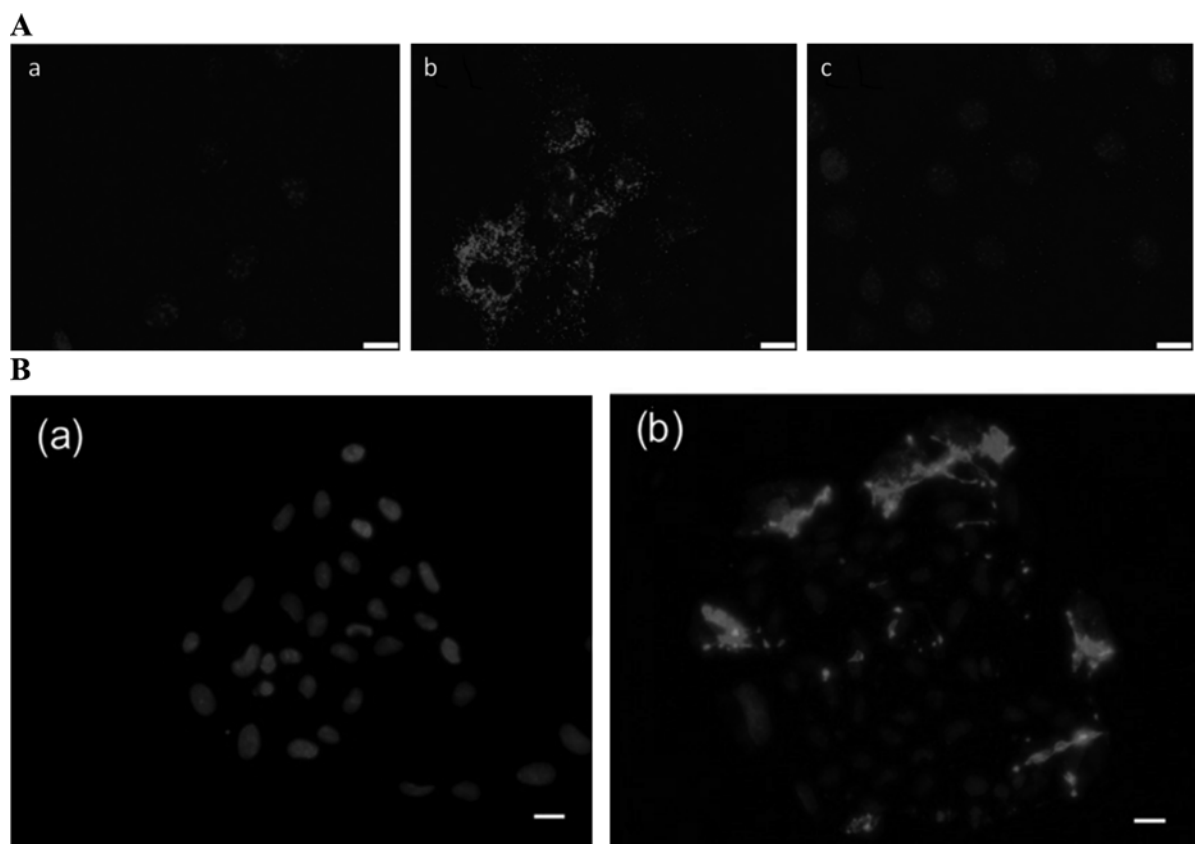

Fig. 5. A) Fluorescent images of EOMA after being incubated for 24 h with 0.5 mg/ml of (a) LTSL; (b) LTSL-cRGD; (c) LTSL-HIT; DAPI (blue), Rhodamine-labeled Liposomes (red). Scale bar: 20 μm. B) Fluorescent images of rGECs after incubation with (a) LTSL and (b) LTSL-HIT (0.5 mg/ml) for 24 h.; (red: rhodamine, liposomes; blue: DAPI, nuclei, scale bar: 20 μm). (For interpretation of the references to colour in this figure legend, the reader is referred to the web version of this article.)
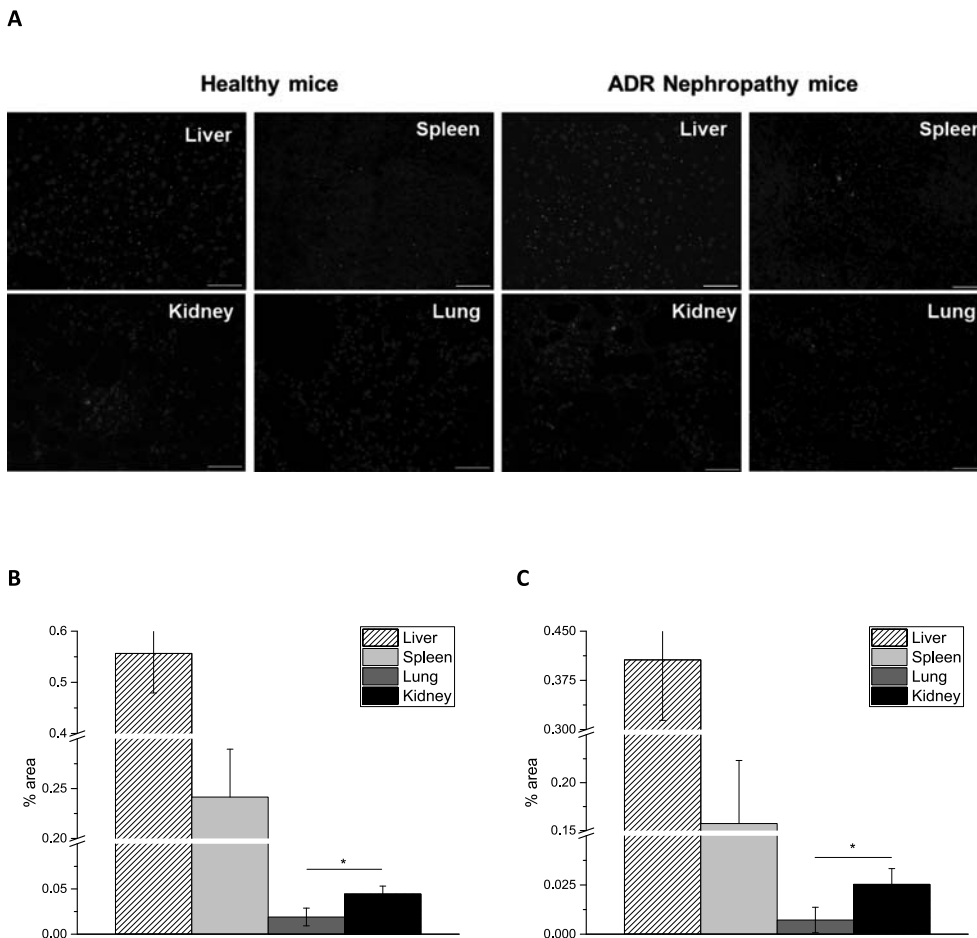
Fig. 6. A) Presentation of fluorescence in tissues from different organs (liver, spleen, lung, kidney) of mice with/without ADRN, after injection of rhodamine-labeled LTSL-HIT (red: rhodamine, liposomes; blue: DAPI, nuclei). Percentage of the rhodamine positivity area (from 10 images of each sample, *p < 0.05), for healthy mice (B) and ADRN mice (C). (For interpretation of the references to colour in this figure legend, the reader is referred to the web version of this article.)
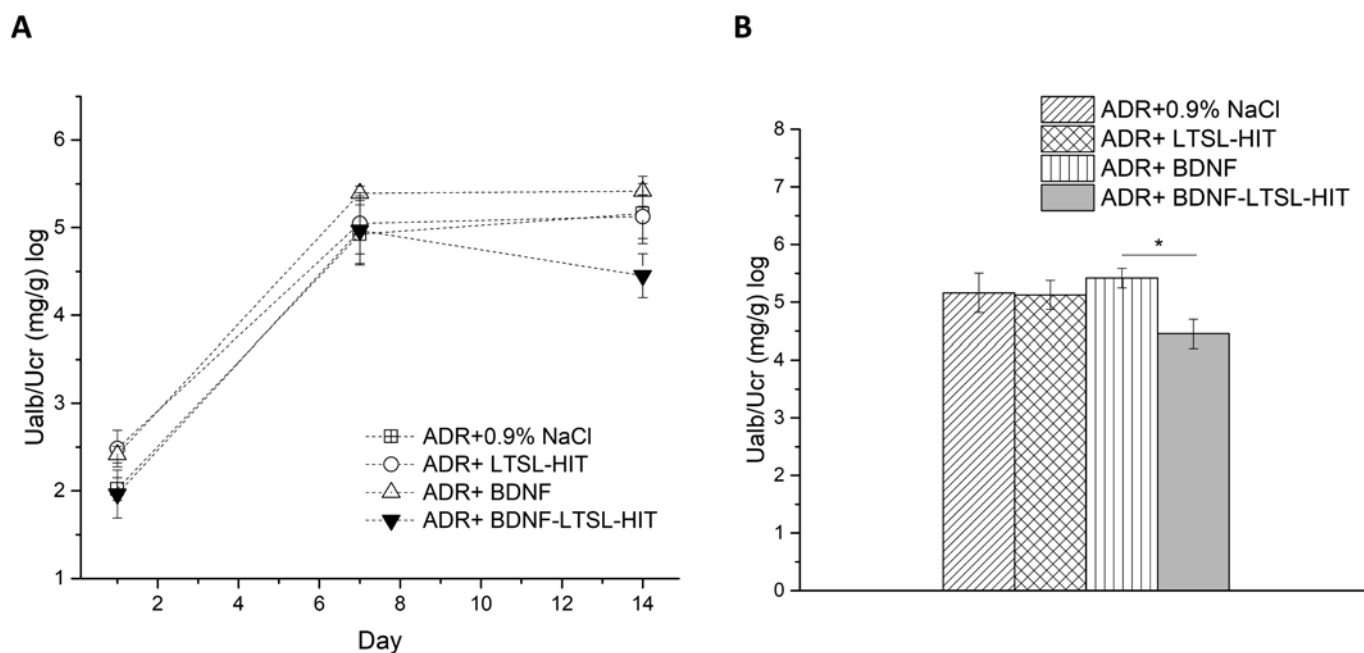

Fig. 7. A) Urinary albumine/creatinine ratio measured at day 1, 7, and 14, after ADR injection. Mice were randomized to receive vehicle (0.9 % NaCl), LTSL-HIT, free BDNF, and BDNF-LTSL-HIT, from day 8 to day 10 (5 mice/group) for a total dosage of 60 μg BDNF /mouse, and finally sacrificed on day 14. B) Albumine/creatinine ratio measured at day 14 (*p < 0.05).
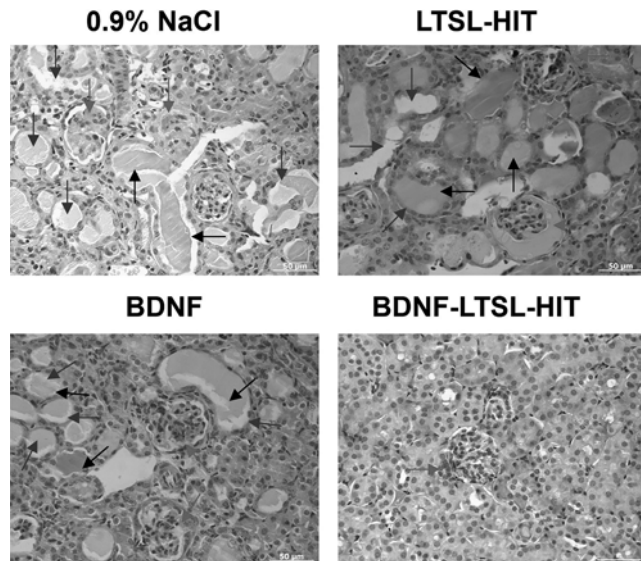
Fig. 8. Histological examination (hematoxylin-eosin staining) of the kidneys following BDNF treatment in ADRN mice, with sacrifice at day 14. Focal and segmental glomerular damage (red arrows), dilated tubules (green arrows), tubular protein casts (black arrows). Scale bars = 50 μm. (For interpretation of the references to colour in this figure legend, the reader is referred to the web version of this article.)

dilation, tubular protein casts, and almost normal glomerular structure except for some hyper-cellularity.

4. Discussion

The LTSL formulation was selected for this study since its relatively low gel-liquid crystal transition temperature (Tm = 40.9 °C) due to the presence of lysolipid Lyso-PC(de Smet et al., 2010; Huang et al., 2017). This allowed to encapsulate BDNF at mild temperature, minimizing its denaturation during the manufacturing process, and retaining the payload at the physiological temperature, with the advantage of a possible rapid release with the addition of mild hyperthermia(Al-Ahmady and Kostarelos, 2016; Huang et al., 2017). The incorporation of PEGylated lipid DSPE-PEG2000 also allowed to improve membrane stability and stealth character for in vivo applications(Huang et al., 2017). The lipid film hydration and extrusion process provided unilamellar liposomes with an ideal particle size for prolonged circulation in vivo (average hydrodynamic diameter ~ 150 nm)(Beltrán-Gracia et al., 2019). The BDNF loading and the encapsulation efficiency were in agreement with previous studies(Huang et al., 2017), and the colloidally stability of these nanocarriers was maintained for at least one month. The manufacturing process, which include heating steps and freeze--thaw cycles, did not significantly affect BDNF stability and activity, as highlighted by SDS-PAGE analysis and the clear demonstration of cytoskeleton repair in cultures of damaged podocytes. These results demonstrated that BDNF was effectively released from liposomes and still retained its activity after encapsulation.

The efficacy of these nanocarriers as BDNF delivery systems in vitro was assessed through a functional evaluation of albumin permeability across a GFB-mimicking barrier (Li et al., 2020; Li et al., 2016). This assay is based on a previously developed podocyte-endothelial cell co-culture device that presents a permeable membrane separating the podocyte and endothelial cell layers.

The addition of BDNF-LTSL suspension to the podocyte compartment resulted in a marked decrease in BSA permeability at 24–48 h. This reduction was a consequence of BDNF release and the repair of the podocyte layer, previously damaged by ADR pre-treatment. Conversely, the addition of liposomes to the endothelial compartment produced only

a limited effect, which may be attributed to the lack of liposome permeation to the podocyte compartment and possibly to partial BDNF uptake by endothelial cells once the protein was released from the lipid vesicles.

In a real intravenous administration of liposomes, these nanocarriers will be transported to the glomerular capillaries of the kidney, where they should encounter the endothelial layer first. To enhance targeting, we therefore explored the possibility of functionalizing liposomes with a homing peptide for the glomerular endothelium. Our investigation focused on the impact of liposome conjugation with targeting peptides on their physicochemical properties, bioactivity, and their interaction with endothelial cells.

Since cRGD was reported to be capable of enhancing the interaction of liposomes with endothelial cells(Schiffelers et al., 2003) through αvβ3 integrin binding(Amin et al., 2015; Danhier et al., 2012; Song et al., 2017), this peptide was initially chosen for in vitro testing due to its ready availability. The inclusion of a thiol cysteine residue enabled the conjugation of cRGD to maleimide-bearing liposomes using sulfhydryl–maleimide coupling chemistry(Koning et al., 2004; Oswald et al., 2016), which was optimised through HPLC analysis to maximize conversion and select the optimal grafting density, ensuring sufficient adhesion to endothelial (EOMA) cell cultures, while providing loading of active BDNF.

When BDNF-LTSL-cRGD suspension was added to the endothelial compartment of the GFB co-culture system, the liposomal uptake by endothelial cells limited the podocyte repairing effect, taking into account that the nanocarriers were too large to cross the co-culture barrier and reach the podocyte layer. On the other hand, when BDNF release was achieved by thermoresponsive degradation of the liposomes at 42 °C, the repairing effect was satisfactory. This suggested that the targeted liposomes in vivo may require a faster BDNF release than the cellular uptake to achieve an efficient repair of podocytes in the GFB, and that a hyperthermia approach may enhance the overall efficacy of the treatment.

To achieve in vivo translation of this liposomal drug delivery system, conjugation of LTSL with HIT peptide was carried out. LTSL-HIT clearly demonstrated specific interaction with rGECs, while showing poor adhesion to non-glomerular endothelial cells (EOMA) in vitro. Therefore, LTSL-HIT were utilized as a model of the in vivo glomerular target.

Afterwards, LTSL-HIT were studied for biodistribution in healthy and ADRN mice after intravenous injection. Both groups showed major sequestration in the liver and spleen, due to the well-known clearance effect of MPS(Allen et al., 1995; Kelly et al., 2011; Lucas et al., 2017). Kidney presence was more noticeable than in the lungs, which may be ascribed to the targeting effect of the HIT peptide.

The therapeutic potential of BDNF encapsulated in HIT-conjugated liposomes was finally explored in vivo using a reduced dosage compared to a previous study on the administration of free BDNF. Treatments on ADRN mice with injections from days 8 to 10, indicated that free BDNF and empty LTSL-HIT were ineffective in reducing proteinuria at day 14, while BDNF-LTSL-HIT showed a modest but discernible decrease in the urinary albumin/creatinine ratio. The limited efficacy aligns with the relatively low accumulation of liposomes in kidney glomeruli, as highlighted by the biodistribution tests. Histological examination also confirmed that BDNF-LTSL-HIT ameliorated kidney damage, evident in reduced tubular dilation and protein casts, and near-normal glomerular structure, while LTSL-HIT and free BDNF had no significant impact.

5. Conclusions

This study offers insights into a potential therapeutic approach involving the liposomal nanodelivery of BDNF for kidney disorders.

BDNF was successfully encapsulated in low temperature sensitive liposomes, ensuring stability and biological activity. BDNF-LTSL effectively repaired F-actin cytoskeleton damage in podocytes and reduced

albumin permeability in a podocyte-endothelial cell co-culture model, indicating its potential for restoring podocyte function. Furthermore, liposomes conjugated with targeting peptide cRGD (BDNF-LTSL-cRGD) enhanced endothelial cell adhesion and uptake without compromising BDNF activity, emphasizing the importance of targeted delivery. Similarly, BDNF-LTSL conjugated with the HIT targeting peptide (LTSL-HIT) exhibited specificity for glomerular endothelial cells, suggesting its potential for in vivo kidney targeting. Biodistribution studies in mice confirmed kidney accumulation of HIT-conjugated liposomes, with promising therapeutic effects observed in ADR nephropathy models. Despite limited kidney accumulation, BDNF-LTSL-HIT treatment resulted in reduced proteinuria and improved kidney histology.

While the BDNF-LTSL-HIT system shows promise as a therapeutic protein delivery system, there are notable limitations typical of active targeted liposomal formulations. Achieving precise targeting remains challenging, as ligand-receptor interactions at the glomerular endothelium may lack the required specificity or selectivity. Biological barriers, such as the mononuclear phagocyte system (MPS), can impede effective delivery to the target site. Despite these challenges, future investigations on the triggered release of BDNF, utilizing local hyperthermia, may be conducted, capitalizing on the thermoresponsive character of the designed formulation.

CRediT authorship contribution statement

Xiaoyi Huang: Writing – review & editing, Methodology, Investigation. **Min Li:** Writing – review & editing, Methodology, Investigation. **Maria Isabel Martinez Espinoza:** Writing – review & editing, Methodology, Investigation. **Cristina Zennaro:** Writing – review & editing, Methodology, Investigation. **Fleur Bossi:** Methodology. **Caterina Lonati:** Methodology. **Samanta Oldoni:** Methodology. **Giuseppe Castellano:** Supervision. **Carlo Alfieri:** Writing – review & editing, Supervision, Conceptualization. **Piergiorgio Messa:** Writing – review & editing, Supervision, Conceptualization. **Francesco Cellesi:** Writing – review & editing, Writing – original draft, Supervision, Methodology, Investigation, Funding acquisition, Data curation, Conceptualization.

Declaration of competing interest

The authors declare that they have no known competing financial interests or personal relationships that could have appeared to influence the work reported in this paper.

Data availability

Data will be made available on request.

Appendix A. Supplementary data

Supplementary data to this article can be found online at https://doi.org/10.1016/j.ijpharm.2024.124322.

References

Al-Ahmady, Z., Kostarelos, K., 2016. Chemical components for the design of temperature-responsive vesicles as cancer therapeutics. Chem. Rev. 116, 3883–3918.

Allen, T.M., Hansen, C.B., Demenezes, D.E.L., 1995. Pharmacokinetics of long-circulating liposomes. Adv. Drug Deliv. Rev. 16, 267–284.

Amin, M., Mansourian, M., Koning, G.A., Badiee, A., Jaafari, M.R., Ten Hagen, T.L.M., 2015. Development of a novel cyclic RGD peptide for multiple targeting approaches of liposomes to tumor region. J. Control. Release 220, 308–315.

Andreska, T., Lüningschrör, P., Sendtner, M., 2020. Regulation of TrkB cell surface expression-a mechanism for modulation of neuronal responsiveness to brain-derived neurotrophic factor. Cell Tissue Res. 382, 5–14.

Badeński, A., Badeńska, M., Świętochowska, E., Didyk, A., Morawiec-Knysak, A., Szczepańska, M., 2022. Assessment of Brain-Derived Neurotrophic Factor (BDNF) concentration in children with idiopathic nephrotic syndrome. Int. J. Mol. Sci.

Barutta, F., Bellini, S., Gruden, G., 2022. Mechanisms of podocyte injury and implications for diabetic nephropathy. Clin. Sci. 136, 493–520.

Beltrán-Gracia, E., López-Camacho, A., Higuera-Ciapara, I., Velázquez-Fernández, J.B., Vallejo-Cardona, A.A., 2019. Nanomedicine review: clinical developments in liposomal applications. Cancer Nanotechnol. 10, 11.

Bruni, R., Possenti, P., Bordignon, C., Li, M., Ordanini, S., Messa, P., Rastaldi, M.P., Cellesi, F., 2017. Ultrasmall polymeric nanocarriers for drug delivery to podocytes in kidney glomerulus. J. Control. Release 255, 94–107.

Cardenas-Aguayo, M.d.C., Kazim, S.F., Grundke-Iqbal, I., Iqbal, K., 2013. Neurogenic and neurotrophic effects of BDNF peptides in mouse hippocampal primary neuronal cell cultures. PLoS One 8, e53596.

Cellesi, F., Li, M., Rastaldi, M.P., 2015. Podocyte injury and repair mechanisms. Curr. Opin. Nephrol. Hypertens. 24, 239–244.

Chaudhry, M., Lyon, P., Coussios, C., Carlisle, R., 2022. Thermosensitive liposomes: a promising step toward localised chemotherapy. Expert Opin. Drug Deliv. 19, 899–912.

Colombo, C., Li, M., Watanabe, S., Messa, P., Edefonti, A., Montini, G., Moscatelli, D., Rastaldi, M.P., Cellesi, F., 2017. Polymer nanoparticle engineering for podocyte repair: from in vitro models to new nanotherapeutics in kidney diseases. ACS Omega 2, 599–610.

Danhier, F., Le Breton, A., Préat, V., 2012. RGD-based strategies to target alpha(v) beta (3) integrin in cancer therapy and diagnosis. Mol. Pharm. 9, 2961–2973.

de Smet, M., Langereis, S., den Bosch, S.v., Grüll, H., 2010. Temperature-sensitive liposomes for doxorubicin delivery under MRI guidance. J. Control. Release 143, 120–127.

Denby, L., Work, L.M., Von Seggern, D.J., Wu, E., Hunt, E., Nicklin, S.A., Baker, A.H., 2006. 21. Peptide-targeted Ad19p-based adenoviral vectors for renal gene delivery. Mol. Ther. 13, S9.

Denby, L., Work, L.M., Seggern, D.J.V., Wu, E., McVey, J.H., Nicklin, S.A., Baker, A.H., 2007. Development of renal-targeted vectors through combined in vivo phage display and capsid engineering of adenoviral fibers from serotype 19p. Mol. Ther. 15, 1647–1654.

Gao, J., Liang, Z., Zhao, F., Liu, X.J., Ma, N., 2022. Triptolide inhibits oxidative stress and inflammation via the microRNA-155-5p/brain-derived neurotrophic factor to reduce podocyte injury in mice with diabetic nephropathy. Bioengineered 13, 12275–12288.

Gasselhuber, A., Dreher, M.R., Partanen, A., Yarmolenko, P.S., Woods, D., Wood, B.J., Haemmerich, D., 2012. Targeted drug delivery by high intensity focused ultrasound mediated hyperthermia combined with temperature-sensitive liposomes: computational modelling and preliminary in vivovalidation. Int. J. Hyperth. 28, 337–348.

Géral, C., Angelova, A., Lesieur, S., 2013. From molecular to nanotechnology strategies for delivery of neurotrophins: emphasis on brain-derived neurotrophic factor (BDNF). Pharmaceutics 5, 127–167.

Gray, B.P., Brown, K.C., 2014. Combinatorial peptide libraries: mining for cell-binding peptides. Chem. Rev. 114, 1020–1081.

Huang, X., Li, M., Bruni, R., Messa, P., Cellesi, F., 2017. The effect of thermosensitive liposomal formulations on loading and release of high molecular weight biomolecules. Int. J. Pharm. 524, 279–289.

Huang, X., Ma, Y., Li, Y., Han, F., Lin, W., 2021. Targeted Drug Delivery Systems for Kidney Diseases. Frontiers in Bioengineering and Biotechnology 9.

Hwang, S.Y., Kim, H.K., Choo, J., Seong, G.H., Hien, T.B.D., Lee, E.K., 2012. Effects of operating parameters on the efficiency of liposomal encapsulation of enzymes. Colloids Surf. B Biointerfaces 94, 296–303.

Immordino, M.L., Dosio, F., Cattel, L., 2006. Stealth liposomes: review of the basic science, rationale, and clinical applications, existing and potential. Int. J. Nanomed. 1, 297–315.

Jahroudi, N., Lynch, D.C., 1994. Endothelial-cell-specific regulation of von Willebrand factor gene expression. Mol. Cell Biol. 14, 999–1008.

Janssen, M.L., Oyen, W.J., Dijkgraaf, I., Massuger, L.F., Frielink, C., Edwards, D.S., Rajopadhye, M., Boonstra, H., Corstens, F.H., Boerman, O.C., 2002. Tumor targeting with radiolabeled αvβ3 integrin binding peptides in a nude mouse model. Cancer Res. 62, 6146–6151.

Kelly, C., Jefferies, C., Cryan, S.A., 2011. Targeted liposomal drug delivery to monocytes and macrophages. J Drug Deliv 727241, 26.

Koning, G.A., Fretz, M.M., Woroniecka, U., Storm, G., Krijger, G.C., 2004. Targeting liposomes to tumor endothelial cells for neutron capture therapy. Appl. Radiat. Isot. 61, 963–967.

Kraemer, R., Baker, P.J., Kent, K.C., Ye, Y., Han, J.J., Tejada, R., Silane, M., Upmacis, R., Deeb, R., Chen, Y., Levine, D.M., Hempstead, B., 2005. Decreased neurotrophin TrkB receptor expression reduces lesion size in the apolipoprotein E-null mutant mouse. Circulation 112, 3644–3653.

Kulkarni, A.A., Vijaykumar, V.E., Natarajan, S.K., Sengupta, S., Sabbisetti, V.S., 2016. Sustained inhibition of cMET-VEGFR2 signaling using liposome-mediated delivery increases efficacy and reduces toxicity in kidney cancer. nanomedicine: nanotechnology. Biology and Medicine 12, 1853–1861.

Lee, S.H., Lee, J.B., Bae, M.S., Balikov, D.A., Hwang, A., Boire, T.C., Kwon, I.K., Sung, H.-J., Yang, J.W., 2015. Current progress in nanotechnology applications for diagnosis and treatment of kidney diseases. Adv. Healthc. Mater. 4, 2037–2045.

Leeuwis, J.W., Nguyen, T.Q., Dendooven, A., Kok, R.J., Goldschmeding, R., 2010. Targeting podocyte-associated diseases. Adv. Drug Deliv. Rev. 62, 1325–1336.

Li, M., Armelloni, S., Zennaro, C., Wei, C., Corbelli, A., Ikehata, M., Berra, S., Giardino, L., Mattinzoli, D., Watanabe, S., Agostoni, C., Edefonti, A., Reiser, J., Messa, P., Rastaldi, M.P., 2015. BDNF repairs podocyte damage by microRNA-mediated increase of actin polymerization. J. Pathol. 235, 731–744.

Li, M., Corbelli, A., Watanabe, S., Armelloni, S., Ikehata, M., Parazzi, V., Pignatari, C., Giardino, L., Mattinzoli, D., Lazzari, L., Puliti, A., Cellesi, F., Zennaro, C., Messa, P., Rastaldi, M.P., 2016. Three-dimensional podocyte-endothelial cell co-cultures: assembly, validation, and application to drug testing and intercellular signaling studies. Eur. J. Pharm. Sci. 86, 1–12.

Li, M., Alfieri, C.M., Morello, W., Cellesi, F., Armelloni, S., Mattinzoli, D., Montini, G., Messa, P., 2020. Assessment of increased glomerular permeability associated with recurrent focal segmental glomerulosclerosis using an in vitro model of the glomerular filtration barrier. J. Nephrol. 33, 747–755.

Liu, J., Boonkaew, B., Arora, J., Mandava, S.H., Maddox, M.M., Chava, S., Callaghan, C., He, J., Dash, S., John, V.T., Lee, B.R., 2015. Comparison of sorafenib-loaded poly (Lactic/Glycolic) acid and DPPC liposome nanoparticles in the in vitro treatment of renal cell carcinoma. J. Pharm. Sci. 104, 1187–1196.

Lucas, A.T., Herity, L.B., Kornblum, Z.A., Madden, A.J., Gabizon, A., Kabanov, A.V., Ajamie, R.T., Bender, D.M., Kulanthaivel, P., Sanchez-Felix, M.V., Havel, H.A., Zamboni, W.C., 2017. Pharmacokinetic and screening studies of the interaction between mononuclear phagocyte system and nanoparticle formulations and colloid forming drugs. Int. J. Pharm. 526, 443–454.

Oroojalian, F., Charbgoo, F., Hashemi, M., Amani, A., Yazdian-Robati, R., Mokhtarzadeh, A., Ramezani, M., Hamblin, M.R., 2020. Recent advances in nanotechnology-based drug delivery systems for the kidney. J. Control. Release 321, 442–462.

Oswald, M., Geissler, S., Goepferich, A., 2016. Determination of the activity of maleimide-functionalized phospholipids during preparation of liposomes. Int. J. Pharm. 514, 93–102.

Ozkan, S., Isildar, B., Ercin, M., Gezginci-Oktayoglu, S., Konukoglu, D., Nesetoglu, N., Oncul, M., Koyuturk, M., 2022. Therapeutic potential of conditioned medium obtained from deferoxamine preconditioned umbilical cord mesenchymal stem cells on diabetic nephropathy model. Stem Cell Res Ther 13.

Pattni, B.S., Chupin, V.V., Torchilin, V.P., 2015. New developments in liposomal drug delivery. Chem. Rev. 115, 10938–10966.

Schiffelers, R.M., Koning, G.A., ten Hagen, T.L.M., Fens, M.H.A.M., Schraa, A.J., Janssen, A.P.C.A., Kok, R.J., Molema, G., Storm, G., 2003. Anti-tumor efficacy of tumor vasculature-targeted liposomal doxorubicin. J. Control. Release 91, 115–122.

Scindia, Y., Deshmukh, U., Thimmalapura, P.R., Bagavant, H., 2008. Anti-alpha8 integrin immunoliposomes in glomeruli of lupus-susceptible mice: a novel system for delivery of therapeutic agents to the renal glomerulus in systemic lupus erythematosus. Arthritis Rheum. 58, 3884–3891.

Singh, M., Ghose, T., Faulkner, G., Kralovec, J., Mezei, M., 1989. Targeting of methotrexate-containing liposomes with a monoclonal antibody against human renal cancer. Cancer Res. 49, 3976–3984.

Song, Z., Lin, Y., Zhang, X., Feng, C., Lu, Y., Gao, Y., Dong, C., 2017. Cyclic RGD peptide-modified liposomal drug delivery system for targeted oral apatinib administration: enhanced cellular uptake and improved therapeutic effects. Int. J. Nanomed. 12, 1941–1958.

Suana, A.J., Tuffin, G., Frey, B.M., Knudsen, L., Mühlfeld, C., Rödder, S., Marti, H.P., 2011. Single application of low-dose mycophenolate mofetil-OX7-immunoliposomes ameliorates experimental mesangial proliferative glomerulonephritis. J. Pharmacol. Exp. Ther. 337, 411–422.

Ta, T., Porter, T.M., 2013. Thermosensitive liposomes for localized delivery and triggered release of chemotherapy. J. Control. Release 169, 112–125.

Wang, Y., Wu, Q., Wang, J., Li, L., Sun, X., Zhang, Z., Zhang, L., 2020. Co-delivery of p38α MAPK and p65 siRNA by novel liposomal glomerulus-targeting nano carriers for effective immunoglobulin a nephropathy treatment. J. Control. Release 320, 457–468.

Whittaker, C.F., Miklich, M.A., Patel, R.S., Fink, J.C., 2018. Medication safety principles and practice in CKD. Clin. J. Am. Soc. Nephrol. 13, 1738–1746.

Xu, X., Costa, A., Burgess, D.J., 2012. Protein encapsulation in unilamellar liposomes: high encapsulation efficiency and a novel technique to assess lipid-protein interaction. Pharm. Res. 29, 1919–1931.

Zhan, W., Gedroyc, W., Xu, X.Y., 2019. Towards a multiphysics modelling framework for thermosensitive liposomal drug delivery to solid tumour combined with focused ultrasound hyperthermia. Biophysics Reports 5, 43–59.

Zhou, J., Li, R., Zhang, J., Liu, Q., Wu, T., Tang, Q., Huang, C., Zhang, Z., Huang, Y., Huang, H., Zhang, G., Zhao, Y., Zhang, T., Mo, L., Li, Y., He, J., 2021. Targeting interstitial myofibroblast-expressed integrin αvβ3 alleviates renal fibrosis. Mol. Pharm. 18, 1373–1385.